Journal of Guidance, Control, and Dynamics
Vol. 28, No. 6, November–December 2005

Engineering Notes

ENGINEERING NOTES are short manuscripts describing new developments or important results of a preliminary nature. These Notes should not exceed 2500 words (where a figure or table counts as 200 words). Following informal review by the Editors, they may be published within a few months of the date of receipt. Style requirements are the same as for regular contributions (see inside back cover).

Calculating Collision Probability for Arbitrary Space-Vehicle Shapes via Numerical Quadrature

Russell P. Patera*
The Aerospace Corporation,
Los Angeles, California 90009-2957

I. Introduction

METHODS to compute space-vehicle collision probability have been developed and presented in earlier publications.[1–5] The contour integration method was developed to improve computational efficiency and handle arbitrary space-vehicle shapes.[3] Although the method has been applied successfully to related problems,[4,5] some analysts might be reluctant to use the method because it involves contour integration rather than the more familiar numerical quadrature. The current work improves on the previous method by reducing the contour integral to a one-dimensional integral and simplifying space-vehicle shape definition. This improved method was found to be easy to implement, computationally efficient, and accurate.

In computing collision probability, each space object is propagated to a point of closest approach. Assuming the relative velocity between the orbital objects at closest approach is very large compared to the effects of their relative acceleration, the relative velocity can be considered constant during the encounter period. A special method was developed to treat cases involving nonlinear relative motion; however, it will not be discussed here.[6,7]

The collision probability is the integral of the relative position error probability density over the volume swept out by the combined hardbody of the two space objects. After integrating the relative position error along the relative velocity vector direction, one obtains a two-dimensional integral over the projection of the combined hardbody on to a plane normal to the relative velocity vector. The previous work reduced this two-dimensional integral to a one-dimensional contour integral about the perimeter of the projected hardbody area.[3] This was achieved by performing a scale change that symmetrized the position error probability density. Because the contour integral is one dimensional, it requires fewer numerical integration steps than the two-dimensional method for comparable accuracy. It was shown that this simplified form significantly reduces computation time[3,4] and enables treatment of asymmetric hardbody shapes including tethers.[5]

Presented as Paper 2004-5218 at the AIAA/AAS Astrodynamics Specialist Conference, Providence, RI, 16–19 August 2004; received 9 November 2004; revision received 12 January 2005; accepted for publication 8 February 2005.

*Senior Engineering Specialist, Mail Stop M4-066, Center for Orbital and Reentry Debris Studies. Member AIAA.

The current implementation involves shifting the origin of the coordinate system to transform the contour integral to a one-dimensional angular integral. Because the integrand contains the definition of the perimeter in functional form, the same integral can be used for any desired hardbody shape. One needs only to define the desired hardbody shape mathematically. This makes implementation easier because definition of the hardbody shape is performed separately and does not alter other portions of the processing.

The algorithm was implemented in a computer program and tested with known results to validate accuracy. It is particularly useful in situations involving numerous evaluations of collision probability, such as maneuver optimization.[4]

II. Analysis

Once two objects are identified to have collision risk, they are propagated to a time near the closest approach time, such that their relative motion is linear. The relative position and velocity near closest approach are used to determine the closest approach distance and the encounter frame. The positive z axis of the encounter frame is opposite in direction to the relative velocity vector. The positive x axis of the encounter is directed from the first object to the second object. The y axis completes the right-handed system.

The combined hardbody radius is obtained by adding the respective hardbody radii of the two space objects. Figure 1 illustrates the position error covariance probability density, combined hardbody, and positions of the respective space objects in the encounter plane. The probability density is centered on the first space object, which is located at the origin of the coordinate system. The axis having the largest position error standard deviation σ_x axis makes an angle α with the x axis, as illustrated in Fig. 1. The combined hardbody is centered on the second space object located on the x axis. The collision probability is the integral of the probability density over the hardbody area as presented in Eq. (1), where P is the collision probability, r is the distance to the hardbody perimeter, and σ is the symmetrized position error standard deviation. Details of the derivation of the probability integral can be found in the original paper[3]:

$$P = \frac{1}{2\pi} \oint_{\text{perimeter}} \left[1 - \exp\left(\frac{-r^2}{2\sigma^2} \right) \right] \mathrm{d}\varepsilon \tag{1}$$

Equation (1) can be converted to a conventional definite integral by changing to polar coordinates centered in the hardbody volume. Let the new coordinate system be centered at $(R,\ 0)$. Points along the

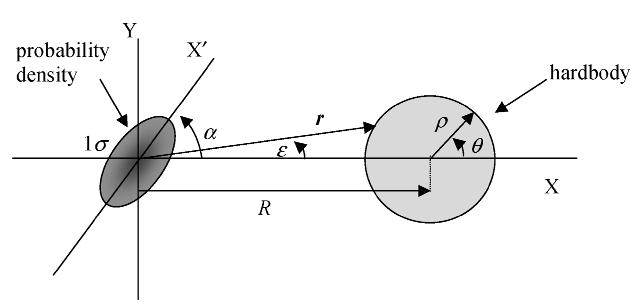

Fig. 1 Hardbody and combined position probability density in encounter plane before symmetrization.

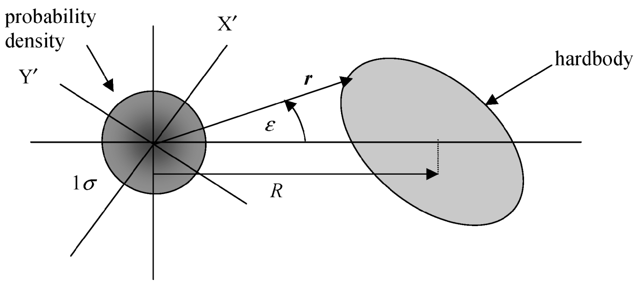

Fig. 2 Deformed hardbody and probability density after symmetrization.

hardbody perimeter are defined as

$$x = R + \rho\cos(\theta), \qquad y = \rho\sin(\theta) \tag{2}$$

where ρ is the radial position of a perimeter point and θ is the angular position as defined in Fig. 1.

A coordinate rotation and scale change transform perimeter points to the symmetrized coordinate frame, as illustrated in Fig. 2:

$$\begin{pmatrix} x' \\ y' \end{pmatrix} = \begin{pmatrix} 1 & 0 \\ 0 & f \end{pmatrix} \begin{bmatrix} \cos(\alpha) & \sin(\alpha) \\ -\sin(\alpha) & \cos(\alpha) \end{bmatrix} \begin{pmatrix} x \\ y \end{pmatrix} \tag{3}$$

where f is the ratio of the x axis $\sigma_{x'}$ to y axis $\sigma_{y'}$, in the diagonal frame.

The contour integration parameter in Eq. (1) ε is related to θ by the relation

$$\tan(\varepsilon) = \frac{y'}{x'} = \frac{f\rho\cos(\alpha)\sin(\theta) - Rf\sin(\alpha) - f\rho\sin(\alpha)\cos(\theta)}{R\cos(\alpha) + \rho\cos(\alpha)\cos(\theta) + \rho\sin(\alpha)\sin(\theta)} \tag{4}$$

which can be written in compact form as

$$\tan(\varepsilon) = \frac{f\rho\sin(\theta - \alpha) - Rf\sin(\alpha)}{R\cos(\alpha) + \rho\cos(\theta - \alpha)} \tag{5}$$

The derivative of Eq. (5) with respect to ε yields

$$\frac{d\varepsilon}{d\theta} = \cos^2(\varepsilon)\frac{d[\tan(\varepsilon)]}{d\theta} = \frac{f\rho^2 + f\rho R\cos(\theta) + Rf\rho'\sin(\theta)}{r^2} \tag{6}$$

where

$$r^2 = \sqrt{x'^2 + y'^2} = [R + \rho\cos(\theta)]^2[\cos^2(\alpha) + f^2\sin^2(\alpha)]$$
$$+ \rho^2\sin^2(\theta)[\sin^2(\alpha) + f^2\cos^2(\alpha)]$$
$$+ 2\rho(1 - f^2)\cos(\alpha)\sin(\alpha)\sin(\theta)[R + \rho\cos(\theta)] \tag{7}$$

and

$$\rho' = \frac{d\rho}{d\theta}$$

Using Eq. (6) in Eq. (1) transforms Eq. (1) from a contour integral to a definite integral given by

$$P = \frac{1}{2\pi}\int_0^{2\pi}\left[\frac{f\rho^2 + Rf\rho\cos(\theta) + Rf\rho'\sin(\theta)}{r^2}\right] \times \left[1 - \exp\left(\frac{-r^2}{2\sigma^2}\right)\right] d\theta \tag{8}$$

If $R = \rho$, r can equal zero, yet the integrand remains finite. In this case, the exponential term in the integrand can be expanded. Keeping the first few terms in the expansion, the integrand becomes

$$[f\rho^2 + Rf\rho\cos(\theta) + Rf\rho'\sin(\theta)](1/2\sigma^2 - r^2/8\sigma^4\cdots) \tag{9}$$

Equation (8) provides an accurate method for computing collision probability very efficiently. For spherical hardbodies, ρ is constant, and the ρ' term vanishes. If ρ varies as a function of θ, the ρ' term is retained. Simple numerical methods enable the integration to be accomplished without the evaluation of trigonometric functions. Therefore, the evaluation of Eq. (8) is extremely efficient. No approximations were used in obtaining Eq. (8). The definite integral form of Eq. (8) can be used in numerical integration packages, thus enabling easy implementation.

Numerical precision can be improved by splitting the integrands in Eqs. (1) and (8):

$$P = \frac{1}{2\pi}\oint_{\text{perimeter}} d\varepsilon - \frac{1}{2\pi}\oint_{\text{perimeter}} \exp\left(\frac{-r^2}{2\sigma^2}\right) d\varepsilon \tag{10}$$

$$P = \frac{1}{2\pi}\oint_{\text{perimeter}} d\varepsilon - \frac{1}{2\pi}\int_0^{2\pi}\left[\frac{f\rho^2 + Rf\rho\cos(\theta) + Rf\rho'\sin(\theta)}{r^2}\right] \times \exp\left(\frac{-r^2}{2\sigma^2}\right) d\theta \tag{11}$$

The first term in Eqs. (10) and (11) is easily evaluated based on the location of the origin with respect to the hardbody area:

$$\frac{1}{2\pi}\oint_{\text{perimeter}} d\varepsilon = \begin{pmatrix} 0, & R > \rho \\ 1, & R < \rho \end{pmatrix} \tag{12}$$

Equation (9) could be used for the special case of $R = \rho$.

III. Numerical Results

Equation (8) was implemented in a computer program and used to evaluate the collision probability for a set of 28 space object test cases having spherical hardbodies, as illustrated in Table 1. For these cases, ρ' is zero, because ρ is constant. The same cases were evaluated using contour integration in Eq. (1). Results from the two methods were in agreement to within 3×10^{-6}% error using only 200 integration steps in Eq. (8). Table 1 also contains closest approach distance and combined hardbody radius.

These same cases were used to check the validity of the ρ' term in Eq. (8) by shifting the origin of ρ as illustrated in Fig. 3. In this

Table 1 Comparison of results

Closest approach, km	Hardbody radius, km	Collision probability	Difference between methods,%
10.30595	0.261429	7.11×10^{-05}	2.57×10^{-06}
11.7910878	0.200077	4.32×10^{-05}	2.57×10^{-06}
5.3875133	0.271668	1.30×10^{-04}	2.56×10^{-06}
7.4893021	0.200515	5.52×10^{-05}	2.57×10^{-06}
34.5054014	0.265202	1.25×10^{-04}	2.58×10^{-06}
3.1965724	0.368366	3.05×10^{-04}	2.55×10^{-06}
75.3755093	0.200401	3.56×10^{-06}	2.56×10^{-06}
59.824544	0.200479	5.54×10^{-06}	2.56×10^{-06}
67.4297582	0.223129	4.55×10^{-06}	2.55×10^{-06}
46.0314966	0.258091	4.01×10^{-06}	2.57×10^{-06}
86.6519575	0.367134	1.06×10^{-05}	2.57×10^{-06}
78.4784936	0.200167	5.08×10^{-06}	2.58×10^{-06}
23.68313	0.300531	1.00×10^{-05}	2.58×10^{-06}
48.9289256	0.200404	3.14×10^{-06}	2.56×10^{-06}
123.6147301	0.200809	2.94×10^{-06}	2.56×10^{-06}
80.1446518	0.200866	6.00×10^{-06}	2.56×10^{-06}
45.2565622	0.200011	5.61×10^{-06}	2.59×10^{-06}
66.0937136	0.200071	1.74×10^{-06}	2.57×10^{-06}
78.3123166	0.200753	2.60×10^{-06}	2.56×10^{-06}
29.4894323	0.200135	4.79×10^{-06}	2.57×10^{-06}
59.9174311	0.261378	5.21×10^{-06}	2.56×10^{-06}
42.6579135	0.203766	6.51×10^{-06}	2.59×10^{-06}
140.0742924	0.200206	2.54×10^{-06}	2.58×10^{-06}
45.2052324	0.200079	3.27×10^{-06}	2.56×10^{-06}
85.4181172	0.200388	3.04×10^{-06}	2.56×10^{-06}
33.9892239	0.200960	2.57×10^{-06}	2.57×10^{-06}
17.6995351	0.200603	3.51×10^{-06}	2.57×10^{-06}
3.9057833	0.299000	1.32×10^{-05}	2.55×10^{-06}

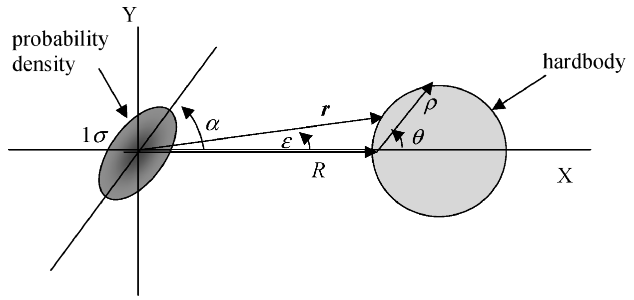

Fig. 3 Alternate parameterization of Eq. (8) with new *R* and ρ definitions.

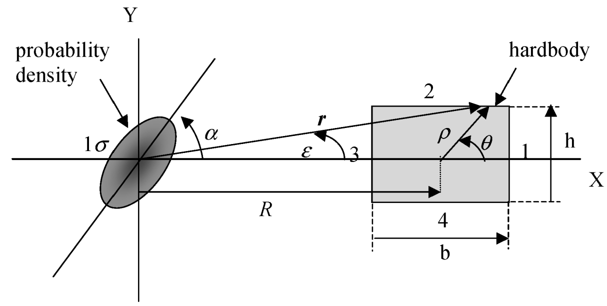

Fig. 4 Rectangular-shaped hardbody used for test cases in Table 2.

case ρ and ρ' are functions of θ, and the limits of integration of Eq. (8) are from $-pi/2$ to $+pi/2$. Thus, the following adjustments were made while using Eq. (8):

$$\tilde{R} = R - \rho, \qquad \tilde{\rho}(\theta) = 2\rho\cos(\theta), \qquad \tilde{\rho}'(\theta) = -2\rho\sin(\theta) \quad (13)$$

Here $\tilde{R}$, $\tilde{\rho}(\theta)$, and $\tilde{\rho}'(\theta)$ are used in place of R, ρ, and ρ' in Eqs. (7) and (8). Using this adjusted formulation on the 28 cases presented in Table 1 resulted in the same collision probabilities. This serves to validate the ability of Eq. (8) to handle asymmetric cases.

The asymmetric algorithm was further validated via comparison with the contour integration method developed earlier.[3] The test cases involve a rectangular-shaped hardbody, as shown in Fig. 4. The functional form of ρ' and ρ' are unique for each side of the rectangle and are given here.

Side 1:

$$\rho = \frac{b}{2\cos(\theta)}, \qquad \rho' = \frac{b\sin(\theta)}{2\cos^2(\theta)} \quad (14)$$

Side 2:

$$\rho = \frac{h}{2\sin(\theta)}, \qquad \rho' = \frac{-h\cos(\theta)}{2\sin^2(\theta)} \quad (15)$$

Side 3:

$$\rho = \frac{-b}{2\cos(\theta)}, \qquad \rho' = \frac{-b\sin(\theta)}{2\cos^2(\theta)} \quad (16)$$

Side 4:

$$\rho = \frac{-h}{2\sin(\theta)}, \qquad \rho' = \frac{h\cos(\theta)}{2\sin^2(\theta)} \quad (17)$$

where b is the base and h is the height of the rectangle in Fig. 4. Equations (14–17) were used in Eq. (8) to compute collision probability for cases illustrated in Table 2. Various parameters were varied in the test cases, as shown in Table 2. The contour integration method was also applied to these test cases and yielded the same values for collision probability. The consistent agreement between the two methods over the various cases indicates that Eq. (8) is valid.

Table 2 Results for rectangle

R, km	σ, km	f	α, deg	Height, km	Base, km	Probability
0.5	50	10	90	0.04	0.04	1.014×10^{-6}
0.5	10	2	90	0.04	0.04	5.067×10^{-6}
0.5	10	2	90	0.04	0.40	5.066×10^{-5}
0.5	50	10	0	0.40	0.04	1.018×10^{-5}
0.5	50	10	0	0.04	0.40	1.019×10^{-5}
0.5	50	10	90	0.20	0.40	5.066×10^{-5}
0.3	50	10	90	0.20	0.40	5.082×10^{-5}
0.8	50	10	90	0.20	0.40	5.027×10^{-5}
0.8	10	10	90	0.20	0.40	9.223×10^{-4}
0.8	9.2824	0.1119	−55.56	0.20	0.40	1.652×10^{-5}

IV. Conclusions

The collision probability contour integral was converted into a definite integral that enables accurate efficient implementation. The method is applicable to both symmetric and asymmetric hardbody shapes. Hardbody shapes are defined using polar coordinates centered in the hardbody. Spherical hardbody shapes have circular projected areas and constant radius ρ, whereas nonspherical shapes require ρ to be a function of the polar angle θ. The collision probability for an arbitrary hardbody shape can be evaluated if ρ and its derivative ρ' are known functions of θ. Because no approximations were made, the error depends only on the fidelity of the particular numerical integration algorithm employed.

The method was implemented in a computer program and compared to known results for spherical and rectangular hardbody shapes. Not only did the current implementation provide correct results, but it was found to have better numerical accuracy than the original contour integral for an equivalent number of integration steps. Assuming the hardbody radius is less than the minimum separation distance at closest approach, the original contour integration parameter $d\varepsilon$ changes sign as one integrates about the contour. The resulting subtraction produces more truncation error than does the current formulation. During integration, ε varies less than the current integration parameter θ. As a result, the current implementation yields greater accuracy with fewer integration steps.

Accuracy, efficiency, and ease of implementation make this collision probability integral a very attractive candidate for collision probability calculations involving linear relative motion.

Acknowledgments

The author thanks L. Andrew Campbell, Val Chobotov, and Justin McNeill for reviewing this Note and providing valuable comments.

References

[1]Alfriend, K. T., Akella, M. R., Lee, D., Frisbee, J., and Foster, J. L., "Probability of Collision Error Analysis," *Space Debris*, Vol. 1, No. 1, 1999, pp. 21–35.

[2]Berend, N., "Estimation of the Probability of Collision Between Two Catalogued Orbiting Objects," *Advances in Space Research*, Vol. 33, No. 1, 1999, pp. 243–247.

[3]Patera, R. P., "General Method for Calculating Satellite Collision Probability," *Journal of Guidance, Control, and Dynamics*, Vol. 24, No. 4, 2001, pp. 716–722.

[4]Patera, R. P., and Peterson, G. E., Space Vehicle Maneuver Method to Lower Collision Risk to an Acceptable Level," *Journal of Guidance, Control, and Dynamics,* Vol. 26, No. 2, 2003, pp. 233–237.

[5]Patera, R. P., "Method for Calculating Collision Probability Between a Satellite and a Space Tether," *Journal of Guidance, Control, and Dynamics*, Vol. 25, No. 5, 2002, pp. 940–945.

[6]Patera, R. P., "Satellite Collision Probability for Nonlinear Relative Motion," *Journal of Guidance, Control, and Dynamics*, Vol. 26, No. 5, 2003, pp. 728–733.

[7]Patera, R. P., "Application of Symmetrized Covariances in Space Conflict Prediction," World Space Congress, PEDAS1-B1.4-0039-02, Oct. 2002.